

Fluid flow and seismicity pattern: Evidence from the 1997 Umbria-Marche (central Italy) seismic sequence

Andrea Antonioli, Davide Piccinini, Lauro Chiaraluce, and Massimo Cocco

Dipartimento di Sismologia e Tettonofisica, Istituto Nazionale di Geofisica e Vulcanologia, Rome, Italy

Received 16 December 2004; revised 29 March 2005; accepted 6 April 2005; published 26 May 2005.

[1] We model the spatial and temporal evolution of seismicity during the 1997 Umbria-Marche seismic sequence in terms of subsequent failures promoted by fluid flow. The diffusion process of pore-pressure relaxation is represented as a pressure perturbation generated by coseismic stress changes and propagating through a fluid saturated medium. The values of isotropic diffusivity range between 22 and 90 m²/s. The calculated value of anisotropic diffusivity ($D_{\text{aniso}} = 250$ m²/s) is largest along the average strike (N140°) direction of activated faults. Our results suggest that the observed spatio-temporal migration of seismicity is consistent with fluid flow. **Citation:** Antonioli, A., D. Piccinini, L. Chiaraluce, and M. Cocco (2005), Fluid flow and seismicity pattern: Evidence from the 1997 Umbria-Marche (central Italy) seismic sequence, *Geophys. Res. Lett.*, 32, L10311, doi:10.1029/2004GL022256.

1. Introduction

[2] Earthquakes generate stress perturbations promoting subsequent events and triggering aftershocks. The most common representation of elastic stress interaction is based on the calculation of Coulomb stress changes caused by earthquake dislocations [e.g., *King and Cocco, 2001*], which is very powerful to map the coseismic induced stress field. Other time dependent processes further modify the induced coseismic stress field, such as afterslip, viscoelastic relaxation of the lower crust and fluid flow. These stress variations occur at different temporal scales. If we restrict our analysis to the aftershock duration, pore-fluid flow may play a dominant role in triggering seismicity [*Nur and Booker, 1972*]. Diffusive processes of pore pressure relaxation in fractured and saturated rocks have been proposed to explain both earthquakes [*Noir et al., 1997; Bosl and Nur, 2002*] and induced seismicity [*Talwani and Acree, 1984*].

[3] In this study we aim to test the hypothesis that the evident migration of seismicity observed during the 1997 Umbria-Marche seismic sequence [*Chiaraluce et al., 2004*] is related to the diffusion of a pore-pressure perturbation in a poro-elastic fluid saturated medium. This time dependent perturbation is produced by the coseismic stress changes caused by a previously occurred mainshock. *Noir et al. [1997]* and *Shapiro et al. [2003]* modeled the spatio-temporal pattern of seismicity observed during an earthquake swarm in the Dobi graben (Central Afar, Africa) and the aftershocks of the Antofagasta (Chile) earthquake, respectively. The Umbria-Marche sequence is characterized by six earthquakes with similar magnitudes ($5 < M_w < 6$).

Five out of six earthquakes occurred in areas of enhanced Coulomb stress by previous main shocks [*Cocco et al., 2000; Nostro et al., 2005*] showing evidences that the spatial pattern of seismicity is consistent with elastic stress interaction. However, the temporal evolution of seismicity shows a peculiar pattern: seismicity migrated and activated the southernmost main fault plane before the occurrence of its impending mainshock [*Chiaraluce et al., 2004*]. Our hypothesis is that elastic stress changes caused by the largest magnitude shocks promoted fluid flow. Although we are aware that other mechanisms can explain the aftershock evolution, we test here if seismicity migration is consistent with pore pressure relaxation.

2. The Seismic Sequence

[4] The 1997 Umbria-Marche seismic sequence consists of six moderate magnitude earthquakes ($5 < M_w < 6$) and thousands of aftershocks that in 40 days activated a ~45 km long, NW-trending, fault system. These seismic events ruptured shallow (1–8 km) normal fault segments, dipping to the SW at $40^\circ \div 45^\circ$. All the main shocks and 70% of the aftershocks show similar focal mechanisms. The sequence is characterized by an evident migration of seismicity (Figure 1) along the strike of the main faults from NW to SE and the progressive activation of adjacent and nearby parallel segments. Seismicity is mostly located on the hanging-wall of main faults and it is absent in the foot-wall. A comprehensive synthesis of this seismic sequence can be found in work by *Chiaraluce et al. [2003, 2004]*.

[5] The two largest events of the sequence (M_w 5.7 and 6.0) struck the Colfiorito area on September 26th (within 9 hours from each other) and ruptured two normal faults with opposite rupture directivity. Seismicity was mainly concentrated in this area until the beginning of October (Figure 1), when two other main shocks occurred on October 3rd and 6th (M_w 5.2 and M_w 5.4). Starting from October 4th seismicity began to migrate towards SE where two other main shocks occurred on October 12th and 14th (M_w 5.2 and 5.6, respectively). The seismogenic volume is elongated in the Apenninic direction and seismicity occurred until November along the whole fault system.

[6] Several features make the study of this sequence particularly interesting: (1) earthquakes were located with the double-difference and cross-correlation technique and the resulting errors are of the order of tens of meters [*Chiaraluce et al., 2003*]; (2) seismicity migrated toward the SE-direction progressively activating the main fault planes before the occurrence of their impending mainshocks [*Chiaraluce et al., 2004*]; (3) the analysis of Coulomb stress changes shows that these normal faults interact with each

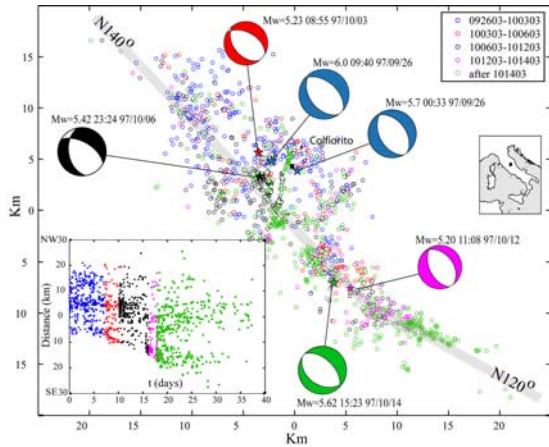


Figure 1. Map showing the Umbria-Marche 1997 seismicity [after Chiaraluce *et al.*, 2004]. The 1520 aftershocks are color-coded by time intervals defined by the occurrence of the six main shocks. The mean strikes of the fault system are reported. The panel shows the space-time diagram of seismicity along a 60 km cross-section oriented N140°.

other [Nostro *et al.*, 2005], but it cannot explain the presence of seismicity in the hanging wall of the main faults [Miller *et al.*, 2004] as well as the temporal migration of seismic events; (4) there are evidence of the presence of fluids in this area [Chiodini *et al.*, 2000]. All these factors motivate our study.

3. Methodology

[7] The modeling of pore-pressure relaxation requires solving the Darcy's equation. In an anisotropic and heterogeneous poro-elastic fluid-saturated medium, the Darcy's law is written as

$$\frac{\partial p}{\partial t} = \frac{\partial}{\partial x_i} \left[D_{ij} \frac{\partial p}{\partial x_j} \right], \quad (1)$$

where D_{ij} are the components of the hydraulic diffusivity tensor, x_j are the components of the vector measuring the distance between the causative perturbation (i.e., the location of the mainshock) and any observation point in the medium; t is the time measured from the origin time of the mainshock (t_0) and p is the pressure. Equation (1) can be derived combining the Darcy's law with the equation of mass conservation for the drained response of a poro-elastic medium [Rice and Cleary, 1976; Shapiro *et al.*, 2003]. Hydraulic diffusivity tensor (D) can be related to permeability tensor (K) using the following relation

$$D = K/\varepsilon\nu C_T, \quad (2)$$

where ε and ν are the rock porosity and the fluid viscosity, respectively, and C_T is the coefficient of the isothermal compressibility.

[8] Equation (1) can be solved for an impulsive pressure pulse represented by a delta function [$p(x, t) = \delta(x)\delta(t)$]. The resulting pore-pressure relaxation has a temporal evolution depending on the square of the distance and the hydraulic

diffusivity [Carslaw and Jaeger, 1959], which can be written for anisotropic diffusivity [Noir *et al.*, 1997] as:

$$t_\alpha = X_\alpha^t D^{-1} X_\alpha \quad (3)$$

where X_α is the vector (of components x_j) measuring the distance between the causative perturbation and each subsequent event of the sequence (indicated by α and t_α is the time separation between these events. Assuming an isotropic diffusivity tensor, equation (3) becomes:

$$t_\alpha = X_\alpha X_\alpha / D_{iso}, \quad (4)$$

where D_{iso} is the isotropic diffusivity value.

[9] Shapiro *et al.* [2003] proposed a solution of the Darcy's law for a step-function point-source pore pressure in a isotropic homogeneous fluid saturated medium. These authors introduced the alternative notion of triggering front to model the spatio-temporal pattern of hydraulically induced seismicity. They propose the following equation defining the triggering front:

$$r = \sqrt{4\pi Dt}, \quad (5)$$

where r is the radius of the triggering front (which is the vector of components x_i), D is the scalar diffusivity ($4D = D_{iso}$) and t is time as in equation (1).

[10] According to the two approaches described above once the pore pressure change reaches a point r at time t , it may trigger an earthquake which occurs in that location at a certain time after the perturbation. In particular, the approach proposed by Shapiro *et al.* [2002] predicts that fluid flow may trigger an earthquake at a location r at any time after the pressure perturbation. Therefore, in a (r, t) plot, seismicity should lie below the parabola defined by equation (5) [see Shapiro *et al.*, 2003]. On the contrary, if earthquake triggering occurs shortly after the pore pressure perturbation (as expected according to the approach proposed by Noir *et al.* [1997]), thus in a (r, t) plot we should observe a relatively narrow parabolic cluster of seismicity along that parabola. Both these approaches measure the distance between hypocenters, thus considering that pore-pressure relaxation begins at the origin time and hypocenters of the causative shock.

4. Application to the Umbria-Marche Sequence

[11] We plot in Figure 2 the triggering front defined by (5) and the Umbria-Marche spatio-temporal aftershocks distribution. Aftershock positions r and origin times t are plotted starting from the September 26th (00:33 UTC M_w 5.7) event. Figure 2 shows that the seismicity distribution agrees with the pore-pressure triggering front envelope predicted by (5) with an isotropic diffusivity of 90 m^2/s : aftershocks lie below the triggering front parabola. We also performed the same calculations for different time intervals identified by the occurrence of subsequent large magnitude ($M_w > 5.2$) main shocks, each of which might be able to modify the pore-pressure field promoting fluid flow. We considered three time intervals: the first comprises seismic events occurred between September 26 and October 6th, when the last main shock struck the Colfiorito area; the

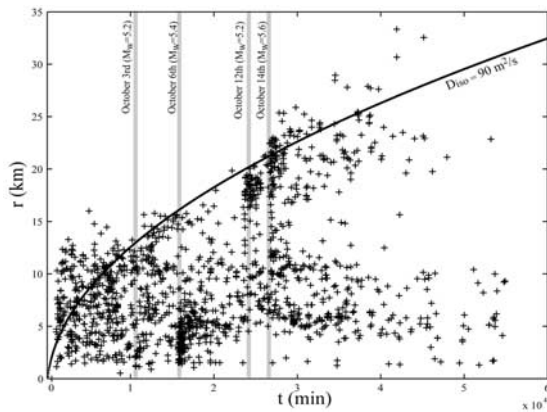


Figure 2. Spatio-temporal distribution of aftershocks. Position and origin time are plotted in distance (r) versus time (t). The black line is the triggering front defined by (5) assuming $D_{iso} = 90 \text{ m}^2/\text{s}$. The gray lines indicate the mainshock occurrence.

second includes events between October 6th and 12th, when seismicity starts to migrate southward, and the last interval includes events occurred after the October 12th (see Figure 1). Therefore, we considered as causative shocks the first September 26th, the October 6th and 12th events. The spatio-temporal evolution of seismicity and the triggering front for these three intervals are shown in Figure 3. We report in Figure 3 only those aftershocks located south of each causative main shock consistently with the observed southeastward seismicity migration. Figure 3 shows that the aftershock evolution for the first and the last time windows is quite consistent with the triggering front hypothesis defined by (5), with a value of hydraulic diffusivity equal to $22 \text{ m}^2/\text{s}$, smaller than that obtained for the whole aftershock sequence ($90 \text{ m}^2/\text{s}$). The fit obtained for the October 6th–12th time window is rather poor. This might be due to the presence in this time window of aftershocks promoted by elastic stress transfer caused by the first September 26th shock, which is located south of the October 6th event.

[12] We performed a test in order to check these results. According to equation (4) we look for a linear relation between time (t_α) and squared distance (X_α^2); if fluid-driven migration exists, we can measure the diffusivity value from the slope of the regression line. In such a way, we model the seismicity migration of those aftershocks which occur immediately or shortly after the pore pressure perturbation at their hypocenters. The linear regression yields an estimate of hydraulic diffusivity equal to $51 \pm 4 \text{ m}^2/\text{s}$, which lies within the range of values estimated above. We have chosen a null hypothesis that consists in verifying if time and squared distance can be fitted by a linear regression with $D_{iso} = 0$. This hypothesis should correspond to a seismicity pattern solely controlled by elastic stress interaction. We used a F-test to verify this hypothesis. Since the obtained F-value exceeds the critical value estimated from the F distribution, we reject the null hypothesis that $D_{iso} = 0$ running a risk of less than 0.1% of being wrong.

[13] This latter approach has the advantage to allow the estimation of anisotropic hydraulic diffusivity values by

applying equation (3) to the aftershock sequence. Assuming that one of the eigenvectors is vertical, the non-diagonal elements D_{xz} and D_{yz} vanish [Noir *et al.*, 1997]. Therefore equation (3) can be written as:

$$t_\alpha = D_{xx}^{-1} X_\alpha^2 + D_{yy}^{-1} Y_\alpha^2 + D_{zz}^{-1} Z_\alpha^2 + 2D_{xy}^{-1} X_\alpha Y_\alpha$$

where D_{ij} are the components of the hydraulic diffusivity tensor. We find the remaining four components of the diffusivity tensor simply imposing a rotation of the reference frame around the vertical axis (z) and looking for the angles that minimize the values of the non-diagonal elements. According to this approach the vertical eigenvector D_{zz} is constant and we find the other two components (D_{xx} and D_{yy}). Figure 4 shows the results of this analysis for the whole sequence. The maximum anisotropic diffusivity value (D_{aniso}) is $275 \text{ m}^2/\text{s}$ and the regression coefficient is 0.7. The maximum eigenvector of the diffusivity tensor is

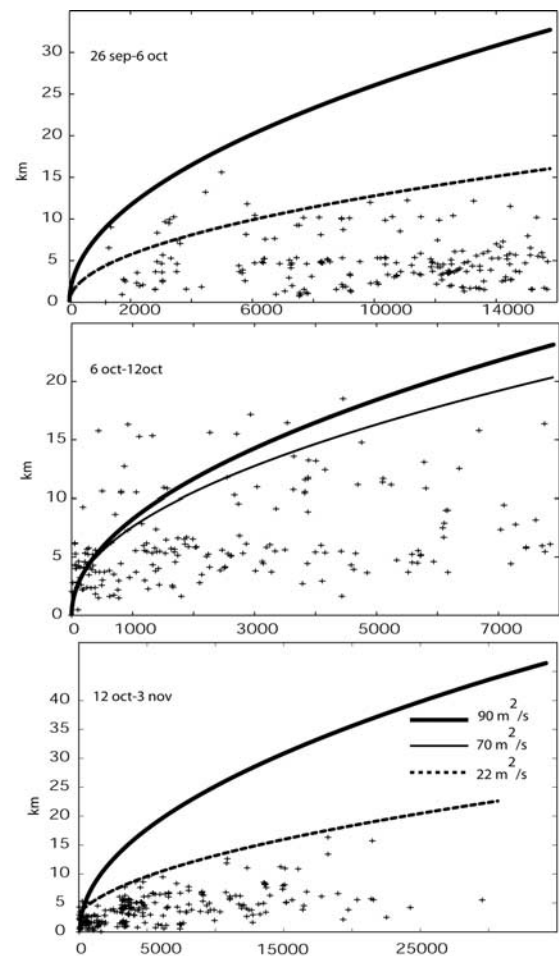


Figure 3. Spatio-temporal distribution of aftershocks in a (r - t) plot for three distinct time windows; the distance in each panel has been computed from different origins (i.e., the causative shocks). The dashed lines and the thin solid line indicate the triggering front defined by (5) for the subsequence and the values of D_{iso} are illustrated in the bottom panel. The thick solid line shows the triggering front associated with the of D_{iso} value estimated for the whole sequence.

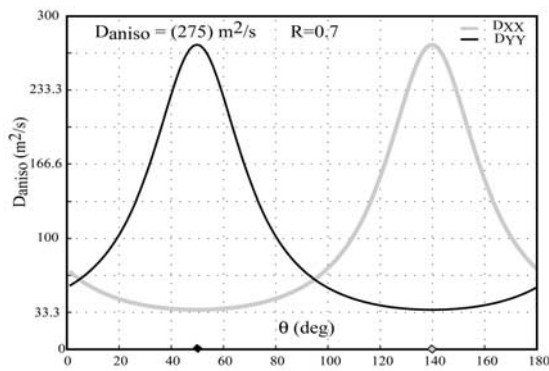


Figure 4. Anisotropic diffusivity as a function of the rotation angle from North direction; gray and black lines represent the D_{xx} and the D_{yy} coefficients, respectively. The directions of maximum diffusivity are indicated by the dots.

oriented N140°, which coincides with the mean strike direction of the major faults (Figure 1).

5. Discussion and Conclusive Remarks

[14] We discuss the hypothesis that the spatial and temporal migration of seismicity observed during the Umbria-Marche sequence is caused by pore pressure relaxation. The fluid flow is modeled in terms of a pore pressure perturbation caused by the coseismic stress changes and propagating in a fluid saturated medium; we estimate isotropic and anisotropic values of hydraulic diffusivity: the former ranges between 22 and 90 m²/s, while the anisotropic diffusivity for the whole sequence is 275 m²/s. Differences between isotropic and anisotropic values were also found by *Noir et al.* [1997]. It is worth noting that the inferred orientation of maximum diffusivity coincides with the average direction of the geological structures in the study area and with the strike of the activated faults: N140° and N120° in the northern and southern portion of the aftershock zone, respectively (Figure 1). The larger value of anisotropic diffusivity might be explained considering that seismicity migrated (at an apparent velocity of 1 km/day) within the damage zone of the active fault system, which is characterized by a higher permeability value [*Miller et al.*, 2004].

[15] Although the inferred values of hydraulic diffusivity vary over one order of magnitude, they lie within the range of values estimated in other areas: they are slightly larger than those obtained in geothermal and tectonic areas, that range between 10⁻² and 10 m²/s [*Talwani et al.*, 1999; *Shapiro et al.*, 1999] and smaller than those estimated by *Noir et al.* [1997] for the central Afar rift (≈10⁴ m²/s). A mean value of 51 m²/s for the hydraulic diffusivity gives for the study area, a permeability value of the order of 7.4×10^{-12} m² [by using $C_t = 2.9 \times 10^{-9}$ Pa⁻¹; $\nu = 10^{-3}$ Pa^{0.5}; $\epsilon = 0.05$]. This value is comparable with the isotropic permeability found by *Miller et al.* [2004] in the same area and much smaller than the permeability (≈10⁻⁸ m²) obtained by *Noir et al.* [1997]. The high diffusivity values can be explained by the presence of high-pressure fluids at depth and by the high permeability of rough fracture at low effective normal stress.

[16] Our interpretation is that pore-pressure relaxation is activated by the coseismic stress changes caused by earth-

quakes. The evidence of intermediate-deep fluid circulation and CO₂ degassing in this portion of the Apennines [*Chiodini et al.*, 2000] further corroborates our results. For this area, *Miller et al.* [2004] proposed that seismicity on the hanging wall of normal faults is promoted by a pressure pulse originating (co-seismically) from this known deep source of trapped high-pressure CO₂ and propagating into the damage region created by the earthquake. Our results suggest that fluid flow and pore pressure relaxation can explain the observed migration of seismicity along the fault strike in the southern portion of the seismogenic volume. The aftershock pattern suggests that triggering of seismicity can be delayed from the computed time of pore pressure perturbation. We emphasize that in complex highly fractured media both elastic and poro-elastic interactions act together in promoting seismicity and controlling its spatial and temporal pattern.

References

- Bosl, W. J., and A. Nur (2002), Aftershocks and pore fluid diffusion following the 1992 Landers earthquake, *J. Geophys. Res.*, *107*(B12), 2366, doi:10.1029/2001JB001155.
- Carslaw, H. S., and J. C. Jaeger (1959), *Conduction of Heat in Solids*, Oxford Univ. Press, New York.
- Chiaraluca, L., W. L. Ellsworth, C. Chiarabba, and M. Cocco (2003), Imaging the complexity of an active normal fault system: The 1997 Colfiorito (central Italy) case study, *J. Geophys. Res.*, *108*(B6), 2294, doi:10.1029/2002JB002166.
- Chiaraluca, L., et al. (2004), Complex normal faulting in the Apennines thrust-and-fold belt: The 1997 seismic sequence in central Italy, *Bull. Seismol. Soc. Am.*, *94*(1), 99–116.
- Chiodini, G., F. Frondini, C. Cardellini, and L. Peruzzi (2000), Rate of diffuse carbon dioxide Earth degassing estimated from carbon balance of regional aquifers: The case of central Apennine, Italy, *J. Geophys. Res.*, *105*, 8423–8434.
- Cocco, M., C. Nostro, and G. Ekstrom (2000), Static stress changes and fault interaction during the 1997 Umbria-Marche earthquake sequence, *J. Seismol.*, *4*, 501–516.
- King, G. C. P., and M. Cocco (2001), Fault interaction by elastic stress changes: New clues from earthquake sequences, *Adv. Geophys.*, *44*, 1–38.
- Miller, S. A., C. Colletini, L. Chiaraluca, M. Cocco, M. Barchi, J. Boris, and P. Kraus (2004), Aftershocks driven by a high-pressure CO₂ source at depth, *Nature*, *427*, 724–727.
- Noir, J., E. Jacques, S. Bekri, P. M. Adler, P. Tapponier, and G. C. P. King (1997), Fluid flow triggered migration of events in the 1989 Dobi earthquake sequence of central Afar, *Geophys. Res. Lett.*, *24*, 2335–2338.
- Nostro, C., L. Chiaraluca, M. Cocco, D. Boumont, and O. Scotti (2005), Coulomb stress changes caused by repeated normal faulting earthquakes during the 1997–1998 Umbria-Marche (central Italy) seismic sequence, *J. Geophys. Res.*, doi:10.1029/2004JB003386, in press.
- Nur, A., and J. R. Booker (1972), Aftershocks caused by pore fluid flow?, *Science*, *175*, 885–887.
- Rice, J. R., and M. P. Cleary (1976), Some basic stress diffusion solutions for fluid saturated elastic porous media with compressible constituents, *Rev. Geophys.*, *14*, 227–241.
- Shapiro, S. A., P. Audigane, and J. J. Royer (1999), Large scale in situ permeability tensor of rocks from induced microseismicity, *Geophys. J. Int.*, *137*, 207–213.
- Shapiro, S. A., E. Rothert, V. Rath, and J. Rindshwenter (2002), Characterization of fluid transport properties of reservoirs using induced microseismicity, *Geophysics*, *67*, 212–220.
- Shapiro, S. A., R. Patzig, E. Rothert, and J. Rindshwenter (2003), Triggering of seismicity by pore-pressure perturbations: Permeability-related signature of the phenomenon, *Pure Appl. Geophys.*, *160*, 1051–1066.
- Talwani, P., and S. Acree (1984), Pore pressure diffusion and the mechanism of reservoir-induced seismicity, *Pure Appl. Geophys.*, *6*, 947–965.
- Talwani, P., J. S. Cobb, and M. F. Schaeffer (1999), In situ measurements of hydraulic properties of a shear zone in northwestern South Carolina, *J. Geophys. Res.*, *104*, 14,993–15,003.

A. Antonioli, L. Chiaraluca, M. Cocco, and D. Piccinini, Dipartimento di Sismologia e Tettonofisica, Istituto Nazionale di Geofisica e Vulcanologia, via di Vigna Murata, 605, Rome I-00143, Italy. (chiaraluca@ingv.it)